Science of the Total Environment 784 (2021) 147148

Contents lists available at ScienceDirect

Science of the Total Environment

journal homepage: www.elsevier.com/locate/scitotenv

Detoxification of oil refining effluents by oxidation of naphthenic acids using TAML catalysts

Angela Pinzón-Espinosa [a,*,1], Terrence J. Collins [b], Rakesh Kanda [a]

[a] Institute of Environment, Health and Societies, Brunel University London, Halsbury Building, Kingston Lane, Uxbridge, Middlesex UB8 3PH, United Kingdom
[b] Institute for Green Science, Department of Chemistry, Carnegie Mellon University, 4400 Fifth Avenue, Pittsburgh, PA 15213, United States

HIGHLIGHTS

- Naphthenic acids (NAs) are constituents of crude oil, corrosive and toxic to various organisms.
- NAs are recalcitrant but need to be removed from wastewater before recycling and disposal.
- The up-scaling potential of the treatment technologies developed so far remains low.
- TAML/H_2O_2 achieved 95% removal of model NAs and 4-fold reduction in toxicity in effluents.
- TAML/H_2O_2 achieved comparable results to ozone but under ultra-dilute conditions.

GRAPHICAL ABSTRACT

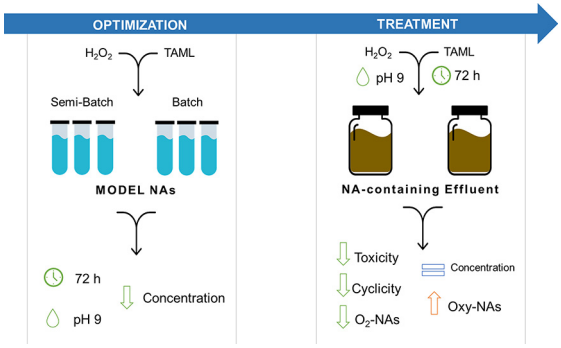

ARTICLE INFO

Article history:
Received 17 February 2021
Received in revised form 9 April 2021
Accepted 10 April 2021
Available online 17 April 2021

Editor: Damia Barcelo

Keywords:
Recalcitrant naphthenic acids
Aliivibrio fischeri
Up-scaling
Oil sands process-affected waters (OSPW)
Hydrogen peroxide
Detoxification

ABSTRACT

The environmental problem stemming from toxic and recalcitrant naphthenic acids (NAs) present in effluents from the oil industry is well characterized. However, despite the numerous technologies evaluated for their destruction, their up-scaling potential remains low due to high implementation and running costs. Catalysts can help cutting costs by achieving more efficient reactions with shorter operating times and lower reagent requirements. Therefore, we have performed a laboratory investigation to assess iron-TAML (tetra-amido macrocyclic ligand) activators to catalyze the oxidation of NAs by activating hydrogen peroxide — considered environmentally friendly because it releases only water as by-product — under ultra-dilute conditions. We tested Fe-TAML/H_2O_2 systems on (i) model NAs and (ii) a complex mixture of NAs in oil refining wastewater (RWW) obtained from a refining site in Colombia. Given the need for cost-effective solutions, this preliminary study explores sub-stoichiometric H_2O_2 concentrations for NA mineralization in batch mode and, remarkably, delivers substantial removal of the starting NAs. Additionally, a 72-h semi-batch process in which Fe-TAML activators and hydrogen peroxide were added every 8 h achieved 90–95% removal when applied to model NAs (50 mg L^{-1}) and a 4-fold reduction in toxicity towards *Aliivibrio fischeri* when applied to RWW. Chemical characterization of treated RWW showed that Fe-TAML/H_2O_2 treatment (i) reduced the concentration of the highly toxic O_2 NAs, (ii) decreased cyclized constituents in the mixture, and (iii) preferentially degraded higher molecular weight species that are typically resistant to biodegradation. The experimental findings, together with the recent development of new TAML catalysts that are far more effective than the TAML catalysts deployed herein, constitute a foundation for cost-effective treatment of NA-contaminated wastewater.

* Corresponding author at: Institute of Environment, Health and Societies, Brunel University London, Kingston Lane, Uxbridge, Middlesex UB8 3PH, United Kingdom.
E-mail address: angelapinzon@itopf.org (A. Pinzón-Espinosa).
[1] Present address: ITOPF, 1 Oliver's Yard, 55 City Road, EC1Y 1DT London, United Kingdom.

https://doi.org/10.1016/j.scitotenv.2021.147148

1. Introduction

Naphthenic acids (NAs, Fig. 1) are natural constituents of crude oil and bitumen, with the general formula $C_nH_{2n-z}O_2$, where n = number of C atoms and Z = hydrogen deficiency (Table S1). NAs are major corrosive agents of process equipment (Slavcheva et al., 1999) and toxic to aquatic organisms (Thomas et al., 2009; Jie et al., 2015; Scarlett et al., 2013; Scarlett et al., 2012), and often end up as toxic contaminants in wastewater from the oil sector, especially refining wastewater (RWW) and oil sands process-affected water (OSPW). Currently, most high profile, public environmental concerns of NA-contaminated wastewater relate to OSPW generated during the extraction of bitumen from the oil sands of northern Alberta, Canada. Under Canada's Fisheries act (Goverment of Canada, 1985), it is not allowed to discharge deleterious substances in water, hence a zero-discharge policy is in place for these effluents. Oil sands companies operate under a no-release strategy, resulting in on-site settling ponds of lake-sized proportions used to store OSPW for years, where NA concentrations range between 40 and 120 mg L^{-1} (Holowenko et al., 2001). Considering that NAs have an estimated half-life in nature of 12.8–13.6 years (Han et al., 2009), the need to accelerate their break-down in OSPW has become a priority for both the oil sands industry and Canada (Giesy et al., 2010; Wu et al., 2019).

In the case of RWW, NAs are associated with the refining of acidic crudes. After refining, NAs are released in wastewater and may reach the environment unless appropriate treatment techniques are applied. The removal of NAs from OSPW remains a priority but receives much less attention in the refining sector (Wang et al., 2015; Pinzon-Espinosa and Kanda, 2020), making RWW an important source of NA environmental contamination (Wong et al., 1996). The composition and concentration of NAs in RWW depend on the type of feedstock, the nature of the extraction process, and the degradation profile over space and time (Toor, 2012). NAs have been reported between 2.8 and 11.6 mg L^{-1} in the effluent of RWW treatment (LC-MS, relative to *p*-toluene sulfonate) (Misiti et al., 2013), but can be present at much higher concentrations, as high as 135 mg L^{-1} in RWW resulting from the processing of highly acidic crudes (GC–MS, relative to 1-chlorooctadecane) (Pinzon-Espinosa and Kanda, 2020).

Many methods have been investigated for the clean-up of NA-contaminated wastewater (Wu et al., 2019; Quinlan and Tam, 2015) but there has been limited success with applied technologies developed over the last decade. Biodegradation has proven to be the most cost-effective technique so far but only some NAs are biodegradable under aerobic conditions (Clemente and Fedorak, 2005). Ozonation has proven to increase overall biodegradability (Vaiopoulou et al., 2015; Brown et al., 2013; Brown and Ulrich, 2015; B. Wang et al., 2013), and activated carbon-based adsorption has been shown to remove hydrophobic NAs (Zubot et al., 2012; Kannel and Gan, 2012). However, none of these treatments have advanced to scale to provide solutions for OSPW and RWW NA-contamination. There remains the urgent need for better processes that align with the ideal characteristics of a viable treatment technology, namely high environmental safety, low cost, low energy, mild conditions, and high efficiency. Catalysts can help providing such conditions.

Iron-TAML activators (Fig. 1) of H_2O_2 have evolved through iterative design (Collins et al., 1998) as miniature (≤1% enzyme mass), mechanistically faithful replicas of peroxidase enzymes, but they greatly outperform the enzymes (Wong et al., 1996; Misiti et al., 2013; Collins, 2002). For the oxidation of NAs, this study utilizes Fe-TAML activators **1a** and **1b** (Fig. 1), respectively the best overall TAML catalyst for persistent pollutants and the prototype TAML. While **1b** is ten times less reactive than **1a** (Tang et al., 2016; Popescu et al., 2008), the fact that it is fluorine-free and relatively inexpensive are attractive features that lead us to also evaluate its properties in TAML/H_2O_2 degradation of NAs.

Previous studies with Fe-TAML/H_2O_2-based treatment processes have reported successful removal of a wide variety of organics in wastewater, including estrogenic compounds (Chen et al., 2012; Mills et al., 2015; Shappell et al., 2008), dibenzothiophene derivatives (Mondal et al., 2006), pharmaceuticals (Shen et al., 2011; Somasundar et al., 2018), a molluscicide (Tang et al., 2016; Tang et al., 2017), halogenated phenols (Wang et al., 2017; Gupta et al., 2002), nitrophenols (Kundu et al., 2015), and bisphenol A (Onundi et al., 2017). All these studies report successful removal of contaminants with very low concentrations of TAML activators, typically ≤100 nM and ranging from single digit nM (4 nM) (Onundi et al., 2017) to low μM (50 μM) (Banarjee et al., 2006), which makes them potentially attractive for upscaling purposes. The reported efficiency of Fe-TAML activators in degrading the highly recalcitrant metaldehyde (Tang et al., 2016; Tang et al., 2017), the compound most responsible for regulatory breaches in the UK municipal water treatment industry, suggested that Fe-TAML/H_2O_2 may be aggressive enough to oxidize recalcitrant NAs and contribute to the clean-up and detoxification of NA-containing effluents for recycling and discharge purposes.

Therefore, the purpose of this study has been to investigate the catalytic performance of **1**/H_2O_2 oxidation systems for the transformation of NAs in order to reduce the toxicity of NA-containing effluents. The study was conducted to (i) test **1**/H_2O_2 on model NAs (**NA1** and **NA2**, Fig. 1**)** (Pinzon-Espinosa and Kanda, 2020); (ii) examine the impact of pH on the performance of **1**/H_2O_2 in NA-contaminated water in the range considered relevant for RWW and OSPW (7–9); (iii) test **1**/H_2O_2 on a RWW sample known to contain a complex mixture of NAs, and (iv) undertake toxicity testing of samples treated with **1**/H_2O_2 using the luminescent bacteria test (LBT) based on *Aliivibrio fischeri* to assess toxicity reduction. Bacteria-based tests are known to detect chemicals with several modes of actions, rendering a wide range of detection, and have low requirements of sample. *A. fischeri* comes in the form of a standardized lyophilized reagent providing a low coefficient of variation.

2. Experimental section

2.1. Chemicals and reagents

Model NAs (4-methyl-1-cyclohexanecarboxylic acid and 4-(4-*tert*-butylphenyl)butanoic acid; Fig. 1) were purchased from Sigma-Aldrich. HPLC-grade solvents were obtained from Fisher Chemical. TAML activators (**1a** [538.19 Da] and **1b** [485.27 Da] as orange crystalline Na^+ salts with one axial water ligand and one water of crystallization) were provided by Carnegie Mellon's Institute for Green Science. H_2O_2 (30% w/w) was purchased from Sigma Aldrich and diluted to 0.3% using Milli-Q® water before use. The stock solution (30% w/w) was standardized every 48 h by redox titration ($KMnO_4$, Sigma Aldrich). $Na_2C_2O_4$ for standardization of $KMnO_4$ was purchased from Fisher Chemical. Unbuffered Milli-Q® water was used as reaction medium. The pH of reaction mixtures was adjusted by addition of 0.01 M KOH or 0.01 M HCl. Catalase from bovine liver was obtained from Sigma Aldrich. The Internal standard (IS) solution (1-chlorooctadecane and *o*-terphenyl; 4000 μg mL^{-1} each) was obtained from Restek UK. Phenol and $K_2Cr_2O_7$ for toxicity testing were purchased from Sigma Aldrich. Stock solutions of 17α-ethinylestradiol (EE2) (10 mg L^{-1}) and TAML catalysts (40 mg L^{-1}) were prepared in water and stored at 4 °C. Stock solutions of catalase (500 mg L^{-1}) were prepared in water and stored at 4 °C for a maximum of one week.

2.2. Fe-TAML/H_2O_2 degradation of model NAs

Reactions were performed in 15-mL glass vials containing reaction medium (10 mL), which consisted of a model NA (50 mg L^{-1}: **NA1** = 356 μM, **NA2** = 227 μM) and a TAML catalyst (100 μg L^{-1}: **1a** = 186 nM, **1b** = 206 nM) in MilliQ® water. Oxidation was initiated by the addition of one aliquot of H_2O_2 (0.3%, 134 μL) and conducted either in batch (H_2O_2 and **1** added once at T_0) or semi-batch (H_2O_2 and **1** added every 8 h) processes (Fig. S1). Reactions were conducted in

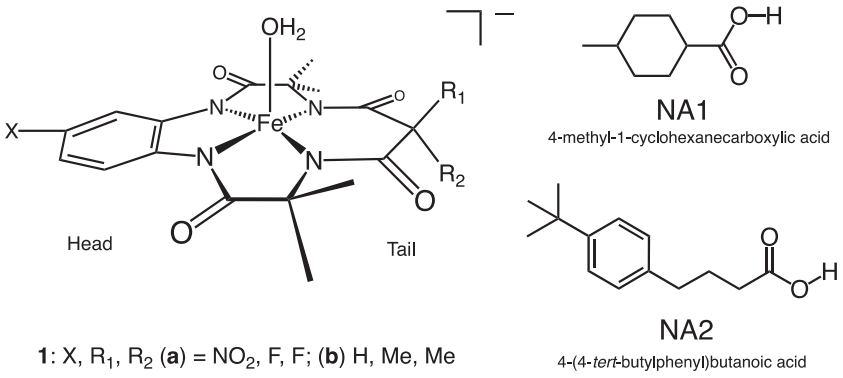

Fig. 1. Structures of Fe-TAML activators (**1a**, **1b**) and model naphthenic acids (**NA1**, **NA2**) used in this study.

triplicate at pH 7, 8, and 9 for 72 h. Quality control of reagents and Fe-TAML activators was performed following the procedure described by Mills et al., 2015 to degrade EE2 (Fig. S2).

The experimental design entailed two controls (NA only, NA + H_2O_2), two catalysts (**1a** and **1b**), and two treatments (batch and semi-batch) for each model NA (**NA1** and **NA2**) at each pH value (7, 8, and 9) (Fig. S1), for a total of 6 test sets and 18 reaction vessels per set. The semi-batch treatment corresponded to one aliquot of H_2O_2 (0.3%, 134 μL) and one of **1**/H_2O_2 (4000 μg L^{-1}, 250 μL) every 8 h, for a total of 9 aliquots. This served as an optimization stage for the subsequent degradation of NAs in RWW samples. For quantification of NAs, aliquots of 500 μL were sampled every 8 h in 2-mL glass vials. An aliquot of catalase solution (500 mg L^{-1}, 50 μL) was transferred to each 2-mL glass vial and left for 5 min to quench the H_2O_2 and stop the reaction. The pH was then lowered by adding HCl (1 M, 50 μL) to allow detection of the NAs acid derivatives via high performance liquid chromatography (HPLC) coupled to a diode array detector (DAD).

2.3. Fe-TAML/H_2O_2 degradation of NAs in RWW

Degradation reactions were conducted in duplicate for 72 h in 500-mL conical flasks containing 200 mL of an RWW sample known to contain NAs (Pinzon-Espinosa and Kanda, 2020). Reactions were initiated by the addition of one aliquot of H_2O_2 (3%, 270 μL) to samples containing TAML catalyst (100 μg L^{-1}: **1a** = 186 nM, **1b** = 206 nM). MilliQ® water, RWW alone, and an uncatalyzed reaction of RWW were used as controls. Reactions were conducted in semi-batch mode, corresponding to 9 added aliquots of H_2O_2 (3%, 270 μL) and **1**/H_2O_2 (40 mg L^{-1}, 500 μL). Reactions were stopped by adding catalase (500 mg L^{-1}, 5 mL) and left for 15 min for quenching. An aliquot (5 mL) was taken from each flask for toxicity tests; the remaining sample underwent liquid extraction *prior* analysis, as described below.

2.4. Liquid-liquid extraction (LLE)

An aliquot of the IS solution (20 μL) was added to post-treatment RWW samples to a final concentration of 100 μg L^{-1} of each component, and the pH was then adjusted to 2 using 1 M HCl. Samples were transferred to separatory funnels and extracted (x3) with dichloromethane (20 mL); the resulting organic extracts were combined and reduced to incipient dryness (a small volume without fully drying them out, hence avoiding evaporative losses of the lower molecular weight compounds) in a TurboVap® LV workstation. Extracts were then split in half and re-dissolved in dichloromethane (100 μL) for analysis via gas chromatography coupled with mass spectrometry (GC–MS) for semi-quantification of naphthenic acids and in methanol (100 μL) for liquid chromatography coupled with high-resolution mass spectrometry (LC-HRMS) for identification of individual congeners within the NA mixture.

2.5. HPLC-DAD analysis

Depletion of model NAs in water was calculated by measuring the residual NAs remaining in the reaction medium after oxidation. Quantification was performed using HPLC-DAD on an Agilent 1260 HPLC instrument (Agilent 1260 pump, Agilent degasser, Agilent DAD, column oven, and auto-sampler) using a Hyperclone® C8 (150 × 2 mm, 5 μm, Phenomenex) column. Mobile phases consisted of HPLC-grade water (A) and acetonitrile (B), pumped at 0.7 mL min^{-1}. Gradient elution was 1% B 0–1 min, ramped to 100% B by 2 min and held until 3 min, returning to 1% B by 4 min and held for 2 min, for a total run of 6 min. Monitoring of **NA1** and **NA2** was carried out at 210 nm (RT: 3.95 min ± 0.01) and 254 nm (RT: 4.11 min ± 0.01), respectively. External calibration solutions were prepared in Milli-Q® water.

2.6. GC–MS analysis

Depletion of NAs in RWW was calculated by semi-quantifying NAs in LLE extracts after treatment with **1**/H_2O_2. Analyzes were conducted using a Perkin Elmer Clarus® 500 instrument equipped with a DB-5 capillary column (30 m × 0.25 mm I.D.) coated with 0.25 μm film 5% phenyl polysilphenylene siloxane. Carrier gas was high-purity helium at 1.0 mL min^{-1}. The inlet was held at 250 °C and injection volume was 1 μL. Column was held at 35 °C for 4 min, ramped at 8 °C/min to 310 °C, and held for 10 min, for a total run time of 48 min. MS was operated in electron ionization mode at 70 eV (scan range 50 to 600 amu). Perfluorotributyl-amine (PFTBA) was used for calibration. Filament emission current was 0.06 pA.

2.7. LC-HRMS analysis

LLE extracts from post-treatment RWW samples were analyzed using HRMS on a Thermo Exactive® mass spectrometer using a Thermo Accela LC pump and a CTC autosampler. Separation was conducted using a Varian Pursuit XRs C18 (100 × 3.0 mm, 3 μm, 100 Å) column. Mobile phases consisted of 0.1% NH_4OH in HPLC water (A) and 0.1% NH_4OH in methanol (B), pumped at 600 μL min^{-1}. Gradient elution was 10% B from 0 min to 2 min, ramped to 70% B by 2.5 min and held until 6 min, ramped to 100% B by 6.5 min and held until 7.5 min, returning to 10% B by 9 min and held for 3 min, for a total run of 12 min. Detection was performed in negative ion mode (scan range 80–500 *m/z*) with the following settings for the heated-electrospray ionization (H-ESI) source: sheath gas flow rate 50 units; spray voltage

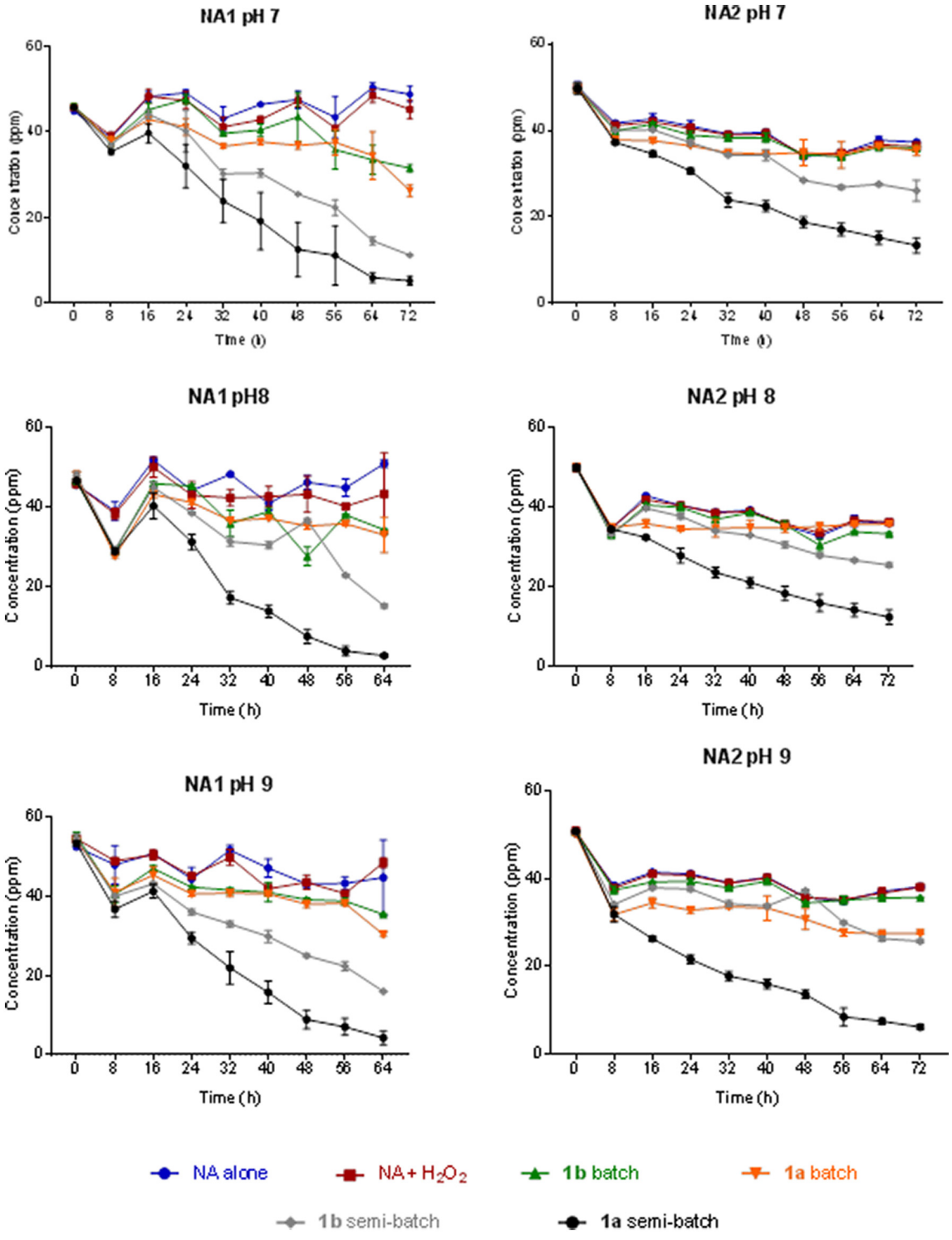

Fig. 2. Temporal dimension of oxidation of model NAs using **1a**/**1b** and H_2O_2 at pH values **Top** 7, **Middle** 8, **Bottom** 9. Conditions: MilliQ® water, total reaction time 72 h, room temperature, NAs (50 mg L^{-1}), **1** (batch: 100 μg L^{-1}, **1a** = 186 nM, **1b** = 206 nM; semi-batch: 900 μg L^{-1}, **1a** = 1674 nM, **1b** = 1854 nM), H_2O_2 (batch: 40 mg L^{-1},1176 μM; semi-batch: 360 mg L^{-1}, 10,584 μM).

4000 V; capillary temperature 350 °C; capillary voltage 55 V; tube lens voltage 105 V; skimmer voltage 26 V; heater temperature 300 °C.

2.8. Toxicity evaluation

Toxicity of aqueous RWW after treatment with **1**/H_2O_2 was measured using a modified version of the LBT methodology described in BS EN ISO 11348-3:2008, adapting the procedure to 96-well plates (Supplementary information – Toxicity evaluation section). Samples were analyzed in duplicate using phenol (400 mg L^{-1} in saline solution) as reference substance (expected EC_{50} = 13–26 mg L^{-1}), saline solution (20% NaCl) as negative control, and Cr(VI) (105.8 mg L^{-1} of $K_2Cr_2O_7$ in saline solution) as positive control. A Promega GloMax™ luminometer was used for light readings, and incubation was performed in an

Aqualytic thermostatic cabinet at 15 °C ± 0.3. EC_{50} values were determined using the linear regression approach.

2.9. Statistical analyzes

Two-way analysis of variance (ANOVA) and the Tukey's multiple comparison test were used to determine significant differences within and between treatments using Prism version 7.03 (Graphpad software, San Diego, CA). Significance level (α) was 0.05.

3. Results and discussion

3.1. Method development

Preliminary reactions with model NAs (50 mg L^{-1}) were conducted with TAML catalysts ranging from 40 to 100 μg L^{-1} (**1a** = 74.4–186 nM, **1b** = 82.4–206 nM) and H_2O_2 from 20 to 100 mg L^{-1} (588–2940 μM) in order to optimize the subsequent stage for removal of NAs in RWW. Decomposition was observed at 100 μg L^{-1} of **1** (**1a** = 186 nM, **1b** = 206 nM) in combination with 40 mg L^{-1} of H_2O_2 (1176 μM), thus these conditions were used for the degradation reactions conducted subsequently.

Results for activity checks of **1a** and **1b** aqueous solutions conducted before **NA** degradation are shown in Fig. S2.

3.2. Performance of Fe-TAML catalysts for the oxidation of model NAs

Due to the particularly high volumes of NA-contaminated wastewater in the oil sector, extreme efficiency is essential to favor low costs and the eventual practicality of any potential real-world process. Thus, this study became all about discovering if effective degradation of NAs could be achieved with relative concentrations of NAs, catalyst, and hydrogen peroxide that would have commercial viability.

Fig. 2 shows the performance of **1a**/H_2O_2 and **1b**/H_2O_2 in the catalytic degradation of **NA1** and **NA2**. Because of the critical importance of the relative amounts of NAs, peroxide, and TAML catalysts, their relative quantities for both batch and semi-batch processes are presented in Table 1 and the resulting molar ratios in Table 2. The peroxide mineralization requirement ($[H_2O_2]/[NA]$) for **NA1** = 21 and for **NA2** = 36, which were exceeded in semi-batch reactions, as observed in Table 2. Oxidation reactions conducted under batch conditions (**1** at 100 μg L^{-1}, **1a** = 186 nM, **1b** = 206 nM; H_2O_2 at 40 mg L^{-1}, 1176 μM) proved to be insufficient to fully degrade model NAs, removing <45% (Table S2). However, it is noteworthy that these reactions were conducted under sub-stoichiometric conditions (Table 2) and, yet TAML catalysts delivered a substantial removal under such demanding circumstances. Further research would be required to understand the mechanistic principles behind these results.

As has been found for metaldehyde, particularly persistent compounds, such as NAs, can be degraded by repeated treatments with TAML/oxidant (Tang et al., 2016). Analysis of semi-batch oxidation reactions revealed that lower final concentrations of model NAs were consistently achieved under **1a**/H_2O_2 vs **1b**/H_2O_2 at all pH values (Fig. 2), which was anticipated due to the increased oxidative aggression provided by the electron-withdrawing capacity of the NO_2 group (Popescu et al., 2008). Moreover, superiority of **1a** over **1b** was statistically significant at all pH values for both NAs (p = 0.9997–<0.0001) (Popescu et al., 2008). As shown in Fig. 2, semi-batch reactions with **1a** achieved degradation rates of approximately 95% for **NA1** and 90% for **NA2** within 72 h, demonstrating the suitability of Fe-TAML/H_2O_2 systems to decompose model NAs under laboratory conditions. The corresponding values with **1b** are 75.6% at pH 7, 68.3% at pH 8, and 70.7% at pH 9 for **NA1**, and 48.4% at pH 7, 49.0% at pH 8, and 49.1% at pH 9 for **NA2**.

3.3. Effect of initial pH on the performance of 1 in catalyzing the oxidative degradation of model NAs by H_2O_2

The catalytic reactivity of TAML activators is highly pH dependent with the highest rates having been found near pH 9 for **1a** and near pH 10 for **1b** for multiple substrates (Collins et al., 2014; Su et al., 2018; Ellis et al., 2010). Previous studies with TAML catalysts have been conducted using buffered solutions as a matrix, but we conducted the oxidation reactions in unbuffered water to approximate real-world water treatment. Degradation took place in milliQ® water with initial pH values of 7, 8, or 9; these pH values were selected based on the native pH of the RWW samples (~7) and the reported pH values for OSPW—typically between 8 and 9 (Toor, 2012)—because these effluents are important sources of NAs into the environment.

The relative catalytic performances of **1a** and **1b** for the degradation of model **NA1** and **NA2** under semi-batch conditions at different pH values is set out in Fig. S3. Data show that initial pH did not have a marked effect on the oxidation of **NA1** with **1a** (α = 0.05; p = 0.8253, 0.7944, 0.4356, pH 7, 8, 9, respectively) or **1b** (α = 0.05; p = 0.7645, 0.3481, 0.7645, pH 7, 8, 9, respectively), or on the oxidation of **NA2** with **1b** (α = 0.05; p = 0.8914, 0.8717, 0.6067). However, **1a** performed significantly better at pH 9 (α = 0.05; p <0.0001, <0.0001) for oxidizing **NA2**.

Previous studies using ozone to oxidize NAs have also reported higher efficiency at basic pH (Perez-Estrada et al., 2011; Afzal et al., 2015), which has been linked to the decomposition of ozone at high pH values and the resulting formation of hydroxyl radicals (•OH) (Perez-Estrada et al., 2011; Glaze et al., 1987). The non-selectivity of •OH plays a key role in the removal of NAs by hydrogen abstraction (Glaze, 1987; Meshref et al., 2017). However, •OH seem not to be significantly involved in Fe-TAML oxidation reactions, and the pH-dependent efficiency is related to the acidity of the axial water ligand which, when deprotonated, promotes the activation of H_2O_2 (Ryabov and Collins, 2009; Ghosh et al., 2003) to form the Fe(V)(oxo)-TAML as the most aggressive reactive intermediate (Ryabov and Collins, 2009; de Oliveira et al., 2007).

3.4. By-product formation from degradation of NA2

HPLC-DAD analysis of the reaction medium after **1a**/H_2O_2 degradation showed the formation of a by-product with increasing peak area over time (Fig. S4), which was not present in untreated samples. LC-HRMS results confirmed the presence of an additional compound that

Table 1
Relative amounts of NAs, H_2O_2, and TAML catalysts during batch and semi-batch reactions.

Reagent		Reaction process	
		Batch	Semi-batch
Model NAs	Concentration	50 mg L^{-1} (**NA1** = 356 μM, **NA2** = 227 μM)	50 mg L^{-1} (**NA1** = 356 μM, **NA2** = 227 μM)
H_2O_2 (0.3%)	Aliquots	1 (134 μL at T_0)	9 (134 μL each, every 8 h)
	Final concentration	40 mg L^{-1} (1176 μM)	360 mg L^{-1} (10,584 μM)
TAML catalyst 1 (4 mg L^{-1})	Aliquots	1 (250 μL at T_0)	9 (250 μL each, every 8 h)
	Final concentration	100 μg L^{-1} (**1a** = 186 nM, **1b** = 206 nM)	900 μg L^{-1} (**1a** = 1674 nM, **1b** = 1854 nM)

Table 2
Molar ratios for [NA]/[**1**] and [H_2O_2]/[NA] after completion of batch and semi-batch processes for the degradation of model NAs.

Molar ratio	Reaction process	
	Batch	Semi-batch
[NA1]/[1a]	1913.0	212.7
[NA1]/[1b]	1728.0	192.0
[NA2]/[1a]	1220.0	135.6
[NA2]/[1b]	1102.0	122.4
[H_2O_2]/[NA1]	3.3	29.7
[H_2O_2]/[NA2]	5.2	46.6

co-eluted with **NA2** in an unresolved peak (Fig. 3). The peak was composed of 3 unresolved peaks corresponding to **NA2** in two isomeric forms (RT: 3.78 and 3.72 min) and the by-product (RT: 3.64 min) with an accurate mass of 233.1181 and a chemical formula of $C_{14}H_{17}O_3$ (4 ppm error). Analysis using NI-ESI-MS/MS in product ion scanning mode showed fragmentation product ions of *m/z* 188.7 and *m/z* 55.0, corresponding to $C_{14}H_{17}O_3$ and leading to the proposed structure in Fig. 4.

This finding aligns with previous studies oxidizing NAs, where classic NAs (O_2) decrease and oxidized species (O_3, O_4, O_5, and O_6) increase (Meshref et al., 2017), indicating oxidation of classic NAs. As a classic NA, **NA2** underwent oxidation under **1a**/H_2O_2 and transitioned from $C_{14}H_{20}O_2$ to $C_{14}H_{17}O_3$.

3.5. Degradation of NAs in RWW using Fe-TAML/H_2O_2

Reactions with model NAs showed the superiority of **1a** over **1b** and the higher catalytic performance of **1a** at pH 9 for degrading **NA2.** Hence, these conditions were tested in an environmental mixture of NAs using an RWW sample collected at a refining site in Colombia. Reactions were conducted at pH 9 for 72 h in a semi-batch process with final concentrations of 900 μg L^{-1} (1674 nM) for **1a** and 360 mg L^{-1} (10,584 μM) for H_2O_2. To determine technical performance, four endpoints were monitored: (i) toxicity as measured by the LBT, (ii) concentration of NAs as determined using total ion chromatograms (TICs) from GC–MS, (iii) relative abundance of classic and oxy-NAs identified using LC-HRMS and, (iv) NA profiles based on *n* values and *Z* families obtained from HRMS data.

Toxicity results confirmed that no toxicity was exerted by the reaction matrix after quenching with catalase. Results also showed that treatment with **1a**/H_2O_2 reduced the toxicity of RWW by 4-fold after only 72 h (Fig. 5). Ozone alone has been reported to reduce toxicity by 3.3-fold, but this required the continuous supply of ozone throughout the reaction (60 min; constant ozone concentration of 25–35 mg L^{-1}

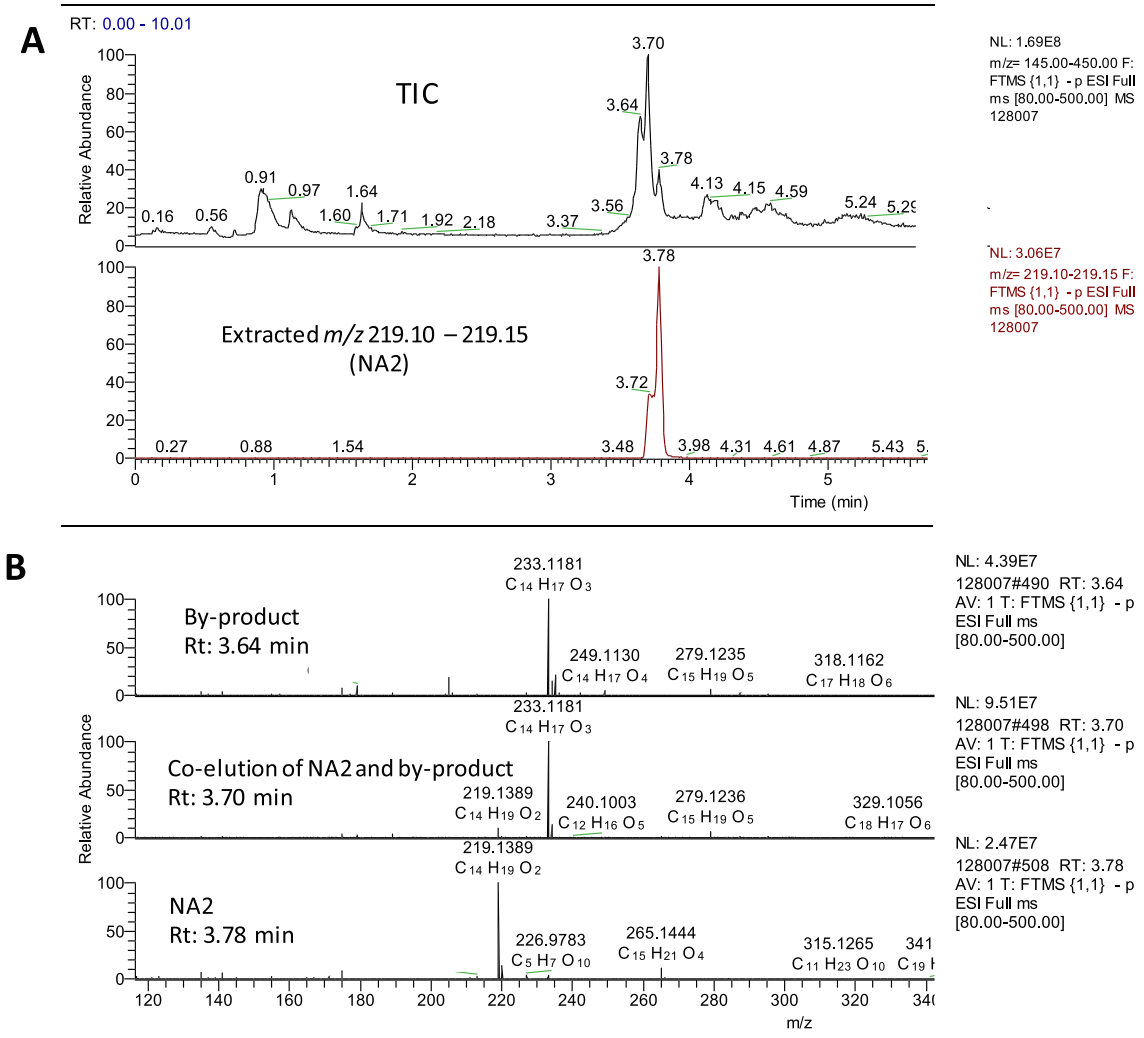

Fig. 3. LC-HRMS results from the reaction medium in semi-batch reactions of NA2 with 1a/H_2O_2 (total reaction time 72 h, room temperature, final concentrations of 900 μg L^{-1} for 1a and 360 mg L^{-1} for H_2O_2). (A) Total ion chromatogram showing an unresolved peak of NA2 and the degradation by-product at 3.72–3.78 min; (B) the high-resolution mass spectra for NA2 and the degradation by-product.

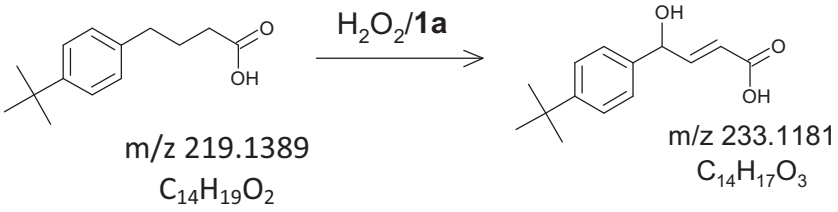

Fig. 4. NA2 and the proposed degradation by-product generated during oxidation reactions with **1a**/H_2O_2. Conditions: semi-batch reaction, total reaction time 72 h, room temperature, final concentrations of 900 μg L^{-1} for 1a and 360 mg L^{-1} for H_2O_2.

in the gas-phase) (Vaiopoulou et al., 2015) implying high operational costs in any scaled-up process.

Semi-quantification of NAs was based on the peak area of the unresolved hump assigned to NAs in GC–MS TICs. The single point external standard method was followed using 1-chlorooctadecane (RSD = 18.3%, spiking concentration 100 μg L^{-1}) as IS for calculation purposes, with the formula below:

$$Concentration\ of\ NAs = \frac{Peak\ area\ of\ NAs}{Peak\ area\ of\ IS} \times Concentration\ of\ IS$$

NAs were estimated to be present in test samples in the concentrations shown in Table 3. These results indicate that the total NA content did not decrease after treatment. However, the reason behind the variability of the untreated and uncatalyzed samples is unclear. These concentration values, however, must be interpreted with caution because the detector does not respond identically to 1-chlorooctadecane and NAs, so an accurate quantitation would require a multiple point standard method using known amounts of the NAs present in the UCM. However, LC-HRMS profiles (Figs. S5 and S6) did show that the semi-batch reaction with **1a**/H_2O_2 changed the distribution and abundance of NA species in RWW, explaining the transformation in toxicological properties regardless of the total NA content.

LC-HRMS analysis revealed that the relative abundance of O_2 NAs decreased after treatment with 1a/H2O2, with significant differences with respect to untreated and uncatalyzed RWW ($\alpha = 0.05$; p = <0.0001), whereas relative abundance of O3 and O4 NAs increased with statistical significance ($\alpha = 0.05$; p <0.0001) (Fig. S5). This finding seems to corroborate the result obtained with **NA2** (Fig. 4), suggesting that semi-batch reactions with **1a** (900 μg L^{-1}, final concentration) and H_2O_2 (360 mg L^{-1}, final concentration) induce the oxidation of O_2 species into oxy-species, which is crucial for the treatment of RWW and OSPW because O_2 NAs have been regarded as the most toxic (Morandi et al., 2015; Yue et al., 2015). Considering that the most probable mode of action for acute toxicity of NAs is narcosis (Frank et al., 2009), which depends on hydrophobicity and size of a molecule, the reduction in toxicity towards *A. fischeri* might be linked to the reduction of hydrophobicity of alkyl groups due to the oxidation of O_2 into O_3 species by **1a**/H_2O_2.

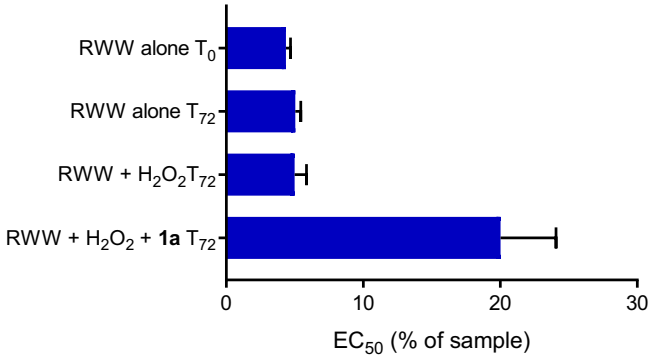

Fig. 5. EC_{50} (% of sample) of treated (semi-batch reaction, total reaction time 72 h, room temperature; **1a** at 900 μg L^{-1} and H_2O_2 at 360 mg L^{-1}, final concentrations) and untreated RWW at T_0 and T_{72} towards *Vibrio fischeri*.

The NA profiles for classic (O_2) and oxy-NAs (O_3, O_4, and O_5) (Fig. S6) revealed that samples undergoing uncatalyzed treatment or no treatment at all showed the same distribution of NA congeners. Treatment with **1a**/H_2O_2 changed the overall profiles of oxy-NAs, with an evident increase in the intensity of O_4 NAs with C11–13 and $Z = -2$, and of $Z = -2$ and -4 in O_5 NAs. Statistical analysis (Fig. 6A) revealed significant differences in $Z = 0, -2, -4$, and -8 for O_3, and $Z = 0, -2, -4, -6$, and -8 for O_4 in treated samples with respect to controls. Overall, relative abundance of species with high Z values declined and those with low Z values increased, possibly due to ring opening (Vaiopoulou et al., 2015; Afzal et al., 2015; Meshref et al., 2017; Scott et al., 2008). This suggests that **1a**/H_2O_2 under the conditions described herein decreased the degree of cyclization of the NA mixture, which follows the trend found with oxidation using electro-oxidation (Abdalrhman et al., 2019) and ozonation (Perez-Estrada et al., 2011). This has important practical implications because cyclization remains a major factor contributing to persistence, with faster biodegradation rates in NA mixtures with lower degrees of cyclization (Han et al., 2008).

As for the carbon content, we used $n = 15$ as margin to classify NAs into low and high molecular weight (MW) (Meshref et al., 2017; Sohrabi et al., 2013) and determine whether treatment with **1a**/H_2O_2 had any effect on high MW species, which are reported to be less biodegradable. As set out in Fig. 6B, both uncatalyzed and catalyzed treatments reduced the relative intensity of high MW species within O_2 NAs from 11% to 4%, which can be linked to oxidation by hydroxyl radicals from H_2O_2. In contrast, low MW NAs in O_3 and O_4 species increased with respect to controls only after treatment with **1a**/H_2O_2, reaching 90% and 43% respectively. In alignment with other oxidation processes (Perez-Estrada et al., 2011; Afzal et al., 2015; Meshref et al., 2017; Abdalrhman et al., 2019), **1a**/H_2O_2 showed preferential oxidation towards high MW NAs, which can be attributed to the increasing number of oxidation sites and H atoms vulnerable to abstraction by hydroxyl radicals (Perez-Estrada et al., 2011).

Table 3
Estimated NA content in RWW samples (untreated, uncatalyzed, catalyzed) using the single point external standard method (IS = 1-chlorooctadecane) for calculation purposes.

Sample	Oxidation conditions	Concentration of NAs (mg L^{-1})
Untreated	None	90 ± 26
Uncatalyzed	Semi-batch reaction Total reaction time 72 h Room temperature (~15 °C) H_2O_2 at 360 mg L^{-1} (final concentration)	87 ± 48
Catalyzed	Semi-batch reaction Total reaction time 72 h Room temperature (~15 °C) H_2O_2 at 360 mg L^{-1} (final concentration) **1a** at 900 μg L^{-1} (final concentration)	133 ± 4

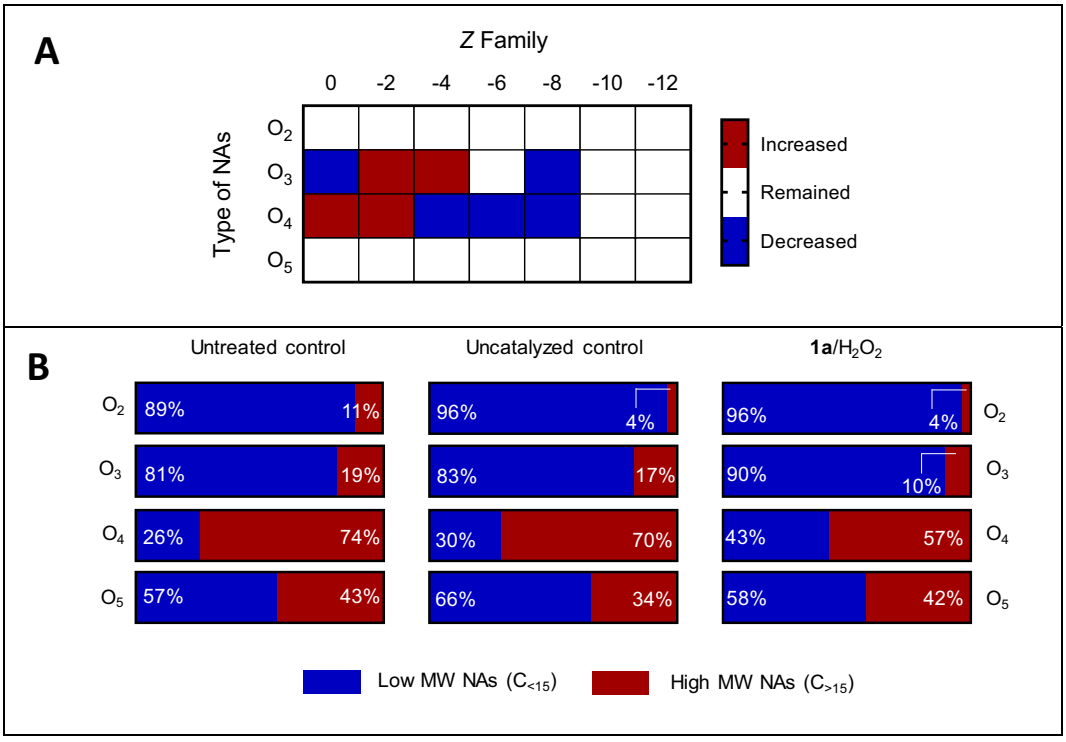

Fig. 6. Changes in the NA mixture in RWW after treatment with **1a**/H_2O_2. A. Heat map showing statistically significant changes in relative abundance of *Z* families for O_2 to O_5 NAs in treated RWW with respect to controls; B. variations in the carbon number of NAs in untreated, uncatalyzed, and catalyzed RWW using C15 as margin to separate NA congeners into low and high MW species.

3.6. Comparison of Fe-TAML/H_2O_2 with other treatment options

Evidence indicates that a combination of chemical oxidation and biological degradation could tackle the complex nature of NAs mixtures and their structure-specific resistance to treatment (Zhang et al., 2019; Martin et al., 2010), but the cost of upscaling such technologies remains the major fallout of this approach. Therefore, catalysts can play a key role in increasing oxidation efficiency, reducing the requirements of reagents and resulting costs. Fe-TAML/H_2O_2 systems are showing a great potential to do so.

Ozone has been reported to be an effective advanced oxidation technology to oxidize model NAs and NAs from OSPW, increasing their biodegradability and reducing toxicity towards *A. fischeri* (Vaiopoulou et al., 2015; Afzal et al., 2015; Hwang et al., 2013; Gamal El-Din et al., 2011). For instance, complete detoxification of OSPW (based on the Microtox® assay) has been achieved after only 50 min of ozonation (Scott et al., 2008). However, when used alone, ozone is frequently applied in semi-batch mode with the gas running continuously (Vaiopoulou et al., 2015; Al-jibouri et al., 2015), thereby providing excess ozone for the duration of the reaction (Scott et al., 2008). The high cost of ozonation (due to the high consumption of energy and ozone) for the large quantities of NA-contaminated wastewater typically produced in the petroleum sector has been acknowledged by previous studies, questioning the economic feasibility of ozone-based technologies for removal of NAs in realistic scenarios (Scott et al., 2008; Gamal El-Din et al., 2011). In fact, effective concentrations of ozone reported in previous research can go up to 150 mg L^{-1} (Afzal et al., 2015; Gamal El-Din et al., 2011; N. Wang et al., 2013). Dosing has been referred to as intensive at concentrations equal or above 80 mg O_3/L, mild at 30–50 mg O_3 L^{-1} (Xue et al., 2016), and light at approximately 25 mg L^{-1} (Vaiopoulou et al., 2015), but even the latter is cost-prohibitive taking into account the large volumes of RWW or OSPW produced daily (Diya'uddeen et al., 2011). For instance, it has been estimated that for municipal wastewater implementing ozonation at 7.7 mg O_3/L with a retention time of 25 min (10 kWh/kg of produced ozone per hour) would increase treatment cost by 0.18–0.22 €/m^3 in the Netherlands and from 0.10–0.18 €/m^3 in Germany (Mulder et al., 2015). It is noteworthy that these costs do not account for recalcitrant contaminants, such as NAs, which might increase operational costs even more. Consequently, ozone alone is hardly applicable for the treatment of RWW or OSPW. Instead, it is now seen as a potential pre-treatment for biological degradation (Xue et al., 2016; Oller et al., 2011) because it targets NAs with greater molecular weight (higher possibility for hydrogen abstraction) and number of rings (more tertiary carbons, which have higher reactivity), which tend to be more resistant to biodegradation (Perez-Estrada et al., 2011; Afzal et al., 2015). Likewise, adsorption has been proposed as a pre-treatment step of ozonation to reduce the levels of applied and utilized ozone (Gamal El-Din et al., 2011).

Our results show the effectiveness of a semi-batch reaction (72 h total reaction time, room temperature (~15 °C)) with **1a** (final concentration 900 μg L^{-1}) and H_2O_2 (final concentration 360 μg L^{-1}) to detoxify RWW by a factor of 4, thereby comparing favorably with a similar approach undertaken previously (Vaiopoulou et al., 2015), where ozone at 25–35 mg O_3/L resulted in a 3.3-fold reduction in toxicity. Further reduction in toxicity towards *A. fischeri* was achieved in the same study when ozone was used in combination with biodegradation, as this approach targets a wide range of NAs, and therefore further work is required to determine if the same benefit can be obtained by using Fe-TAML/H_2O_2 and biodegradation combined. New generations of TAML activators have been developed recently whose catalytic performance is currently under testing for NA degradation and detoxification of NA-contaminated wastewater, aiming at lower concentrations of TAML catalysts and lower requirements of H_2O_2.

4. Conclusions

In this study, we provided an insight into the efficacy of Fe-TAML catalysts (**1a** and **1b**)/H_2O_2 systems to oxidize model NAs and detoxify

RWW containing NAs. It was demonstrated that only very low concentrations of **1a** (900 μg L^{-1}) were required to oxidize aqueous solutions of NAs at high concentration (50 mg L^{-1}), achieving up to 95% degradation of model NAs within 72 h in semi-batch mode. An oxidation by-product revealed hydroxylation of the parent NA by means of LC-HRMS. Catalyst **1a** proved to be superior to **1b**, which is explained by the increased oxidative aggression provided by the electron-withdrawing capacity of the NO_2 group (Popescu et al., 2008; Collins et al., 2014) in its ligand structure.

Treatment with **1a**/H_2O_2 of RWW reduced abundance of O_2 NAs and increased that of oxy-species, reduced degree of cyclization of the NA mixture, and showed preferential oxidation towards high MW NAs. This is comparable with ozonation, which is one of the most effective oxidation technologies for the removal of NAs from OSPW (Quinlan and Tam, 2015; Vaiopoulou et al., 2015; Afzal et al., 2015; Meshref et al., 2017). However, the concentrations of **1a** required for treatment are significantly lower than the required ozone dose to achieve the same results, which is highly relevant for up-scaling purposes. Further work is required to evaluate additional Fe-TAML/H_2O_2 systems in combination with biodegradation to achieve lower residual NAs concentrations in wastewater and lower toxicity. Future studies also need to expand the range of toxicity bioassays to assess the environmental quality of the resulting effluent, and expand on the analysis of by-products, thus providing a more comprehensive study of the fate of NAs after advanced oxidation via Fe-TAML/H_2O_2. Further research is underway to evaluate new generations of Fe-TAML activators aiming at reducing H_2O_2 concentration and reaction times. Overall, our findings suggest that Fe-TAML/H_2O_2 systems are good candidates for reducing the toxicity of effluents containing these pollutants, moving a step forward in water sustainability of the petrochemical sector.

Funding sources

This research was supported by the PhD Scholarship program from COLCIENCIAS (National Department of Science, Technology, and Innovation of Colombia), Grant 568/2012. COLCIENCIAS had no involvement in the design or development of the study, nor in the writing of this manuscript.

CRediT authorship contribution statement

Angela Pinzón-Espinosa: Conceptualization, Investigation, Writing – original draft, Funding acquisition. **Terrence J. Collins:** Writing – review & editing. **Rakesh Kanda:** Conceptualization, Writing – review & editing, Supervision.

Declaration of competing interest

The authors declare that they have no known competing financial interests or personal relationships that could have appeared to influence the work reported in this paper.

Appendix A. Supplementary data

Supplementary data to this article can be found online at https://doi.org/10.1016/j.scitotenv.2021.147148.

References

Abdalrhman, A.S., Ganiyu, S.O., Gamal El-Din, M., 2019. Degradation kinetics and structure-reactivity relation of naphthenic acids during anodic oxidation on graphite electrodes. Chem. Eng. J. 370, 997–1007.

Afzal, A., Chelme-Ayala, P., Drzewicz, P., Martin, J., Gamal El-Din, M., 2015. Effects of ozone and ozone/hydrogen peroxide on the degradation of model and real oil-sands-process-affected-water naphthenic acids. Ozone Sci. Eng. 37, 45–54.

Al-jibouri, A.K., Wu, J., Ranjan Upreti, S., 2015. Ozonation of naphthenic acids in water: kinetic study. Water Air Soil Pollut. 226.

Banarjee, D., et al., 2006. 'Green' oxidation catalysis for rapid deactivation of bacterial spores. Angew. Chem. Int. Ed. 45, 3974–3977.

Brown, L.D., Ulrich, A.C., 2015. Oil sands naphthenic acids: a review of properties, measurement, and treatment. Chemosphere 127, 276–290.

Brown, L.D., et al., 2013. Indigenous microbes survive in situ ozonation improving biodegradation of dissolved organic matter in aged oil sands process-affected waters. Chemosphere 93, 2748–2755.

Chen, J.L., Ravindran, S., Swift, S., Wright, L.J., Singhal, N., 2012. Catalytic oxidative degradation of 17α-ethinylestradiol by FeIII-TAML/H2O2: Estrogenicities of the products of partial, and extensive oxidation. Water Res. 46, 6309–6318.

Clemente, J.S., Fedorak, P.M., 2005. A review of the occurrence, analyses, toxicity, and biodegradation of naphthenic acids. Chemosphere 60, 585–600.

Collins, T.J., 2002. TAML oxidant activators: a new approach to the activation of hydrogen peroxide for environmentally significant problems. Acc. Chem. Res. 35, 782–790.

Collins, T.J., et al., 1998. The design of green oxidants. In: Anastas, P.T., Williamson, T.C. (Eds.), Green Chemistry. Oxford University Press, pp. 46–71.

Collins, T., Khetan, S., Ryabov, A., 2014. Chemistry and applications of iron–TAML catalysts in green oxidation processes based on hydrogen peroxide. Green Catalysis: Homogeneous Catalysis Handbook of Green Chemistry. John Wiley & Sons, pp. 39–77.

Diya'uddeen, B.H., Daud, W.M.A.W., Abdul Aziz, A.R., 2011. Treatment technologies for petroleum refinery effluents: a review. Process. Saf. Environ. Prot. 89, 95–105.

Ellis, W.C., et al., 2010. Designing green oxidation catalysts for purifying environmental waters. J. Am. Chem. Soc. 132, 9774–9781.

Frank, R., et al., 2009. Effect of carboxylic acid content on the acute toxicity of oil sands naphthenic acids. Environ. Sci. Technol. 43, 266–271.

Gamal El-Din, M., et al., 2011. Naphthenic acids speciation and removal during petroleum-coke adsorption and ozonation of oil sands process-affected water. Sci. Total Environ. 409, 5119–5125.

Ghosh, A., et al., 2003. Understanding the mechanism of H+-induced demetalation as a design strategy for robust iron(III) peroxide-activating catalysts. J. Am. Chem. Soc. 125, 12378–12379.

Giesy, J.P., Anderson, J.C., Wiseman, S.B., 2010. Alberta oil sands development. Proc. Natl. Acad. Sci. 107, 951–952.

Glaze, W.H., 1987. Drinking-water treatment with ozone. Environ. Sci. Technol. 21, 224–230.

Glaze, W.H., Kang, J.-W., Chapin, D.H., 1987. The chemistry of water treatment processes involving ozone, hydrogen peroxide and ultraviolet radiation. Ozone Sci. Eng. 9, 335–352.

Goverment of Canada, 1985. Fisheries Act F-14.

Gupta, S. Sen, et al., 2002. Rapid total destruction of chlorophenols by activated hydrogen peroxide. Science (80-.) 296, 326–328.

Han, X., Scott, A., Fedorak, P., Bataineh, M., Martin, J., 2008. Influence of molecular structure on the biodegradability of naphthenic acids. Environ. Sci. Technol. https://doi.org/10.1021/es702220c.

Han, X., MacKinnon, M.D., Martin, J.W., 2009. Estimating the in situ biodegradation of naphthenic acids in oil sands process waters by HPLC/HRMS. Chemosphere 76, 63–70.

Holowenko, F., Mackinnon, M., Fedorak, P., 2001. Naphthenic acids and surrogate naphthenic acids in methanogenic microcosms. Water Res. 35, 2595–2606.

Hwang, G., et al., 2013. The impacts of ozonation on oil sands process-affected water biodegradability and biofilm formation characteristics in bioreactors. Bioresour. Technol. 130, 269–277.

Jie, W., Xiaofeng, C., Yi, H., Xiaoyan, T., 2015. Developmental toxicity and endocrine disruption of naphthenic acids on the early life stage of zebrafish (Danio rerio). J. Appl. Toxicol. 35, 1493–1501.

Kannel, P.R., Gan, T.Y., 2012. Naphthenic acids degradation and toxicity mitigation in tailings wastewater systems and aquatic environments: a review. J. Environ. Sci. Health A 47, 1–21.

Kundu, S., et al., 2015. Rapid degradation of oxidation resistant nitrophenols by TAML activator and H2O2. Catal. Sci. Technol. 5, 1775–1782.

Martin, J.W., et al., 2010. Ozonation of oil sands process-affected water accelerates microbial bioremediation. Environ. Sci. Technol. 44, 8350–8356.

Meshref, M.N.A., Chelme-Ayala, P., Gamal El-Din, M., 2017. Fate and abundance of classical and heteroatomic naphthenic acid species after advanced oxidation processes: insights and indicators of transformation and degradation. Water Res. 125, 62–71.

Mills, M.R., et al., 2015. Removal of ecotoxicity of 17α-ethinylestradiol using TAML/peroxide water treatment. Sci. Rep. 5, 10511.

Misiti, T.M., Tezel, U., Pavlostathis, S.G., 2013. Fate and effect of naphthenic acids on oil refinery activated sludge wastewater treatment systems. Water Res. 47, 460.

Mondal, S., et al., 2006. Oxidation of sulfur components in diesel fuel using Fe-TAML® catalysts and hydrogen peroxide. Catal. Today 116, 554–561.

Morandi, G.D., et al., 2015. Effects-directed analysis of dissolved organic compounds in oil sands process-affected water. Environ. Sci. Technol. 49, 12395–12404.

Mulder, M., Antakyali, D., Ante, S., 2015. Costs of Removal of Micropollutants From Effluents of Municipal Wastewater Treatment Plants - General Cost Estimates for the Netherlands Based on Implemented Full Scale Post-treatments of Effluents of Wastewater Treatment Plants in Germany and Switzerlan.

de Oliveira, F.T., et al., 2007. Chemical and spectroscopic evidence for an FeV-oxo complex. Science (80-.) 315, 835–838.

Oller, I., Malato, S., Sánchez-Pérez, J.A., 2011. Combination of Advanced Oxidation Processes and biological treatments for wastewater decontamination—a review. Sci. Total Environ. 409, 4141–4166.

Onundi, Y., et al., 2017. A multidisciplinary investigation of the technical and environmental performances of TAML/peroxide elimination of Bisphenol A compounds from water. Green Chem. 19, 4234–4262.

Perez-Estrada, L., et al., 2011. Structure-reactivity of naphthenic acids in the ozonation process. Environ. Sci. Technol. 45, 7431–7437.
Pinzon-Espinosa, A., Kanda, R., 2020. Naphthenic acids are key contributors to toxicity of heavy oil refining effluents. Sci. Total Environ., 138119 https://doi.org/10.1016/j.scitotenv.2020.138119.
Popescu, D.-L., et al., 2008. Mechanistically inspired design of Fe III-TAML peroxide-activating catalysts. J. Am. Chem. Soc. 130, 12260–12261.
Quinlan, P.J., Tam, K.C., 2015. Water treatment technologies for the remediation of naphthenic acids in oil sands process-affected water. Chem. Eng. J. 279, 696–714.
Ryabov, A.D., Collins, T.J., 2009. Mechanistic considerations on the reactivity of green Fe (III)-TAML activators of peroxides. Adv. Inorg. Chem. 61, 471–521.
Scarlett, A.G., West, C.E., Jones, D., Galloway, T.S., Rowland, S.J., 2012. Predicted toxicity of naphthenic acids present in oil sands process-affected waters to a range of environmental and human endpoints. Sci. Total Environ. 425, 119–127.
Scarlett, A.G., et al., 2013. Acute toxicity of aromatic and non-aromatic fractions of naphthenic acids extracted from oil sands process-affected water to larval zebrafish. Chemosphere 93, 415–420.
Scott, A.C., Zubot, W., Mackinnon, M., Smith, D.W., Fedorak, P.M., 2008. Ozonation of oil sands process water removes naphthenic acids and toxicity. Chemosphere 71, 156–160.
Shappell, N.W., et al., 2008. Destruction of estrogens using Fe-TAML/peroxide catalysis. Environ. Sci. Technol. 42, 1296–1300.
Shen, L.Q., et al., 2011. Rapid, biomimetic degradation in water of the persistent drug sertraline by TAML catalysts and hydrogen peroxide. Environ. Sci. Technol. 45, 7882–7887.
Slavcheva, E., Shone, B., Turnbull, A., 1999. Review of naphthenic acid corrosion in oilrefining. Br. Corros. J. 34, 125–131.
Sohrabi, V., Ross, M.S., Barker, J.W., 2013. Potential for in situ chemical oxidation of acid extractable organics in oil sands process affected groundwater. Chemosphere 11, 2698–2703.
Somasundar, Y., et al., 2018. Structural, mechanistic, and ultradilute catalysis portrayal of substrate inhibition in the TAML-hydrogen peroxide catalytic oxidation of the persistent drug and micropollutant, propranolol. J. Am. Chem. Soc. 140, 12280–12289.
Su, H., et al., 2018. Quantitative structure–activity relationship for the oxidation of aromatic organic contaminants in water by TAML/H2O2. Water Res. 140, 354–363.
Tang, L.L., et al., 2016. TAML/H2O2 oxidative degradation of metaldehyde: pursuing better water treatment for the most persistent pollutants. Environ. Sci. Technol. 50, 5261–5268.
Tang, L.L., et al., 2017. Homogeneous catalysis under ultradilute conditions: TAML/NaClO oxidation of persistent metaldehyde. J. Am. Chem. Soc. 139, 879–887.
Thomas, K.V., Langford, K., Petersen, K., Smith, A.J., Tollefsen, K.E., 2009. Effect-directed identification of naphthenic acids as important in vitro xeno-estrogens and antiandrogens in North Sea offshore produced water discharges. Environ. Sci. Technol. 43, 8066–8071.
Toor, N.S., 2012. Degradation and Aquatic Toxicity of Oil Sands Naphthenic Acids Using Simulated Wetlands. University of Saskatchewan, Canada.
Vaiopoulou, E., Misiti, T.M., Pavlostathis, S.G., 2015. Removal and toxicity reduction of naphthenic acids by ozonation and combined ozonation-aerobic biodegradation. Bioresour. Technol. 179, 339–347.
Wang, B., Wan, Y., Gao, Y., Yang, M., Hu, J., 2013a. Determination and characterization of oxy-naphthenic acids in oilfield wastewater. Environ. Sci. Technol. 47, 9545–9554.
Wang, N., et al., 2013b. Impact of ozonation on naphthenic acids speciation and toxicity of oil sands process-affected water to Vibrio fischeri and mammalian immune system. Environ. Sci. Technol. 47, 6518–6526.
Wang, B., et al., 2015. Occurrences and behaviors of naphthenic acids in a petroleum refinery wastewater treatment plant. Environ. Sci. Technol. 49, 5796–5804.
Wang, C., Gao, J., Gu, C., 2017. Rapid destruction of tetrabromobisphenol A by iron(III)-tetraamidomacrocyclic ligand/layered double hydroxide composite/H2O2 system. Environ. Sci. Technol. 51, 488–496.
Wong, D., van Compernolle, R., Nowlin, J., O'Neal, D., Johnson, G., 1996. Use of supercritical fluid extraction and fast ion bombardment mass spectrometry to identify toxic chemicals from a refinery effluent adsorbed onto granular activated carbon. Chemosphere 32, 1669–1679.
Wu, C., De Visscher, A., Gates, I.D., 2019. On naphthenic acids removal from crude oil and oil sands process-affected water. Fuel 253, 1229–1246.
Xue, J., Zhang, Y., Liu, Y., Gamal El-Din, M., 2016. Treatment of raw and ozonated oil sands process-affected water under decoupled denitrifying anoxic and nitrifying aerobic conditions: a comparative study. Biodegradation 27, 247–264.
Yue, S., Ramsay, B.A., Wang, J., Ramsay, J., 2015. Toxicity and composition profiles of solid phase extracts of oil sands process-affected water. Sci. Total Environ. 538, 573–582.
Zhang, L., Zhang, Y., Gamal El-Din, M., 2019. Integrated mild ozonation with biofiltration can effectively enhance the removal of naphthenic acids from hydrocarbon-contaminated water. Sci. Total Environ. 678, 197–206.
Zubot, W., Mackinnon, M., Chelme-Ayala, P., Smith, D.W., Gamal El-Din, M., 2012. Petroleum coke adsorption as a water management option for oil sands process-affected water. Sci. Total Environ. 427–428, 364–372.